Polymer Degradation and Stability 167 (2019) 10–20

Contents lists available at ScienceDirect

Polymer Degradation and Stability

journal homepage: www.elsevier.com/locate/polydegstab

A DOPO based reactive flame retardant constructed by multiple heteroaromatic groups and its application on epoxy resin: curing behavior, thermal degradation and flame retardancy

Qianqian Zhang [c], Shuang Yang [a, b, *], Jun Wang [b, c], Jianwen Cheng [c], Qiaoxin Zhang [a, b], Guoping Ding [a, b], Yefa Hu [a, b], Siqi Huo [d]

[a] School of Mechanical and Electronic Engineering, Wuhan University of Technology, Wuhan, 430070, People's Republic of China
[b] Institute of Advanced Material Manufacturing Equipment and Technology, Wuhan University of Technology, Wuhan, 430070, People's Republic of China
[c] School of Materials Science and Engineering, Wuhan University of Technology, Wuhan, 430070, People's Republic of China
[d] Center for Future Materials, University of Southern Queensland, Toowoomba, 4350, Australia

ARTICLE INFO

Article history:
Received 23 April 2019
Received in revised form
16 June 2019
Accepted 20 June 2019
Available online 22 June 2019

Keywords:
Epoxy resin
Flame retardant
Curing behavior
Heteroaromatic
Pyrolysis behavior

ABSTRACT

A high-efficiency flame retardant composed of phosphaphenanthrene, benzothiazole and imidazole groups (PBI) was synthesized and served as flame retardant co-curing agent to reduce the fire hazard of epoxy resin (EP). The chemical structure of PBI was characterized by Fourier transform infrared spectroscopy (FTIR), high-resolution mass spectroscopy (HR-MS), ^{1}H and ^{31}P nuclear magnetic resonance (NMR). The curing behavior, thermal stability and flame retardant properties of the prepared EP systems were investigated. The curing behavior study disclosed that PBI accelerated the crosslinking reaction of EP and was chemically bonded with EP matrix to obtain intrinsic flame retardant thermoset. The resulting EP thermosets showed only slight decrease in glass transition temperature (T_g). The thermogravimetric analysis (TGA) results indicated both the catalytic decomposition and catalytic charring effects of PBI demonstrated by decreased thermal stability and enhanced charring capability of EP/DDS/PBI thermosets. The combustion test results showed remarkable improvement in the flame retardant properties of EP/DDS/PBI thermosets. When the phosphorus content was only 0.75 wt%, EP/DDS/PBI-0.75 thermoset achieved a limiting oxygen index (LOI) value of 34.6% and passed UL94 V-0 rating. Moreover, the peak of heat release rate (pk-HRR), average of heat release rate (av-HRR) and total heat release (THR) values were decreased by 48.7%, 31.1% and 28.3%, respectively, in comparison with those of the EP/DDS thermoset. The flame retardant effect of PBI on EP was attributed to the catalytic charring effect to form protective char layer in condensed phase and release of free radicals with quenching effect and nonflammable gases with diluting effect in gaseous phase.

1. Introduction

Epoxy resin (EP) has been widely applied in diverse industrial fields due to its excellent comprehensive performance. Unfortunately, the intrinsic flammability of EP severely limits its applications in the fields with high flame-resistance requirement [1,2].

Generally, halogen compounds have been widely developed to endow polymer materials with satisfactory flame retardancy. Unfortunately, halogenated flame retardants have come under increased scrutiny due to their potential health and environmental hazards [3,4]. Under this consideration, halogen-free flame retardants have been widely explored and applied to EP [5–7]. Thereinto, phosphorus-based compounds are identified as one of the most promising halogen-free flame retardants, since they are effective radical trappers and efficient charring agents, and exert flame-retardant effect in both gaseous and condensed phases [8–13]. As important categories of phosphorus-based flame retardants, 9,10-dihydro-9-oxa-10-phosphaphenanthrene-10-oxide (DOPO) and its derivatives have received considerable attention due to their facile molecular design and outstanding flame retardant efficiency [14–20]. Recently, many efforts have been devoted

* Corresponding author. School of Mechanical and Electronic Engineering, Wuhan University of Technology, 122 Luoshi Road, Hongshan District, Wuhan, 430070, People's Republic of China.
E-mail address: ysfrp@whut.edu.cn (S. Yang).

https://doi.org/10.1016/j.polymdegradstab.2019.06.020
0141-3910/

to construct synergistic flame-retardant systems through combining different flame retardant elements or functional groups in order to further improve the flame-retardant efficiency without deteriorating other properties of materials. Owing to the high reactivity of DOPO and its derivatives with varying functional groups, a series of synergistic flame-retardant systems such as DOPO/cyclotriphosphazene [21–23], DOPO/triazine [24,25], DOPO/maleimide [26,27], DOPO/triazine-trione [28,29], DOPO/thiazole [30], DOPO/phosphate [31] and DOPO/siloxane [32–35], have been successfully prepared and achieved the expected goal. Hence, it is meaningful to design and synthesize such DOPO based flame retardants composed of multifunctional groups. The ongoing research concerning further development of more simple preparation methods and efficient molecular structures of flame retardants would certainly promote the wider application of flame retardant EP in key fields.

In this work, a high-efficiency flame retardant composed of phosphaphenanthrene, benzothiazole and imidazole groups (PBI) was synthesized via a facile one-pot reaction and used as flame retardant co-curing agent to reduce the fire hazard of EP. The chemical structure of PBI was characterized by FTIR, HR-MS, ^{1}H and ^{31}P NMR. The curing behavior of the EP systems with the presence of PBI was investigated by non-isothermal differential scanning calorimetry (DSC) test. The thermal properties of epoxy thermosets were investigated by TGA and DSC tests. The flame retardant properties of epoxy thermosets were investigated by LOI, UL-94 and cone calorimeter tests. Moreover, the flame retardant mechanism was detailed investigated in gaseous and condensed phases.

2. Experimental

2.1. Materials

1H-Imidazole-4-carbaldehyde, 4,4′-diamino-diphenyl sulfone (DDS), 2-aminobenzothiazole, 9,10-dihydro-9-oxa-10-phosphaphenanthrene-10-oxide (DOPO) and dimethylformamide (DMF) were obtained from Aladdin Reagents (Shanghai) Co., Ltd. Diglycidyl ether of bisphenol-A (DGEBA) with an epoxide equivalent weight (EEW) of about 188 g/equiv was provided by Yueyang Baling Huaxing Petrochemical Co., Ltd. All the reagents were used as received.

2.2. Synthesis of PBI

PBI was synthesized via a facile one-pot reaction. 1H-Imidazole-4-carbaldehyde (4.8 g, 0.05 mol), 2-benzothiazolamine (7.5 g, 0.05 mol) and DMF (150 ml) were introduced to a 250 ml, three-necked and round-bottom glass flask equipped with a mechanical stirrer, reflux condenser and thermometer. The mixture was stirred at 90 °C for 3 h. Afterwards, DOPO (10.8 g, 0.05 mol) was added into the flask, and the mixture was stirred at 90 °C for additional 8 h. Then the mixture was distilled to remove DMF, the crude product was washed for 3 times with ethanol, and then vacuum-dried at 60 °C for 10 h (Yield: 95%). Element analysis (%): C: 62.12 (cal 62.16), H: 3.88 (cal 3.83), N: 12.65 (cal 12.61), S: 7.22 (cal 7.21), O: 7.18 (cal 7.21). The synthesis route was shown in Scheme 1.

2.3. Preparation of EP thermosets

All the details of formula are listed in Table 1. The amount of active protons in PBI and DDS was equal to the amount of epoxy groups in DGEBA.

DGEBA and DDS were blended at 125 °C until a homogeneous solution was obtained. Then the solution was cooled down to 80 °C, and PBI was added. The mixture was further stirred at 80 °C for 10 min to obtain homogeneous solution. Afterwards, the mixture was degassed under vacuum and poured directly into a preheated mold and thermally cured in an air convection oven at 160 °C for 2 h and 180 °C for 4 h.

2.4. Preparation of EP curing systems for non-isothermal DSC test

DGEBA, DDS and PBI were thoroughly blended at room temperature according the formulas shown in Table 1. Moreover, EP/PBI curing system was prepared by mixing DGEBA with PBI (weight ratio: 100: 10) at room temperature.

2.5. Characterization

Fourier Transform Infrared (FTIR) spectra were obtained using a Nicolet 6700 infrared spectrometer (Thermo Fisher Scientific, US). The powdered samples (PBI or the char residues from cone calorimeter test) were thoroughly mixed with KBr and then pressed into pellets. The wavenumber range was set from 4000 to 500 cm^{-1}.

^{1}H and ^{31}P NMR spectra were obtained on a Bruker AV400 NMR spectrometer (Bruker, US) using DMSO-d_6 as the solvent and tetramethylsilane (TMS) as the internal standard.

Mass spectroscopy (MS) was conducted on an Agilent LC-MS 1100 instrument (Agilent, US). High-resolution MS data were recorded on a Thermo Fisher Scientific LTQ FT Ultra instrument.

Elemental analysis (EA) was performed on a Vario EL cube Elemental Analyzer (Elementar, Germany). The contents of carbon (C), hydrogen (H), nitrogen (N), sulphur (S) and oxygen (O) of PBI

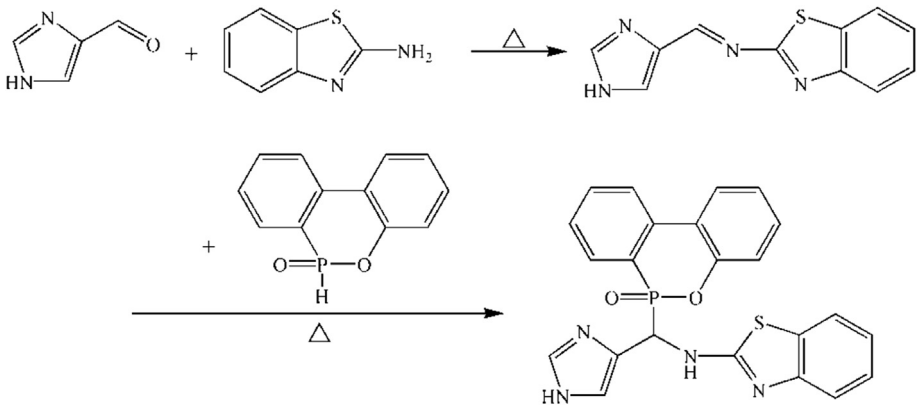

Scheme 1. Synthesis route of PBI.

Table 1
Formulas of the prepared EP thermosets.

Sample code	DGEBA (g)	DDS (g)	PBI (g)	PBI content (wt%)	phosphorus content (wt%)
EP/DDS	100	33.0	0	0	0
EP/DDS/PBI-0.25	100	31.5	4.9	3.6	0.25
EP/DDS/PBI-0.5	100	30.1	10.0	7.1	0.5
EP/DDS/PBI-0.75	100	28.6	15.5	10.8	0.75
EP/DDS/PBI-1.0	100	27.0	21.2	14.3	1.0

were measured.

Differential scanning calorimetry (DSC) thermograms were recorded with PerkinElmer DSC 4000 (PerkinElmer, US) to investigate the non-isothermal curing behavior of the EP mixtures and the glass transition behavior of the cured EP thermosets. The EP mixtures and the cured EP thermosets (approximately 7.0 mg) were put in an alumina crucible and heated from 40 °C to 300 °C at a heating rate of 10 °C/min under N_2 atmosphere with a flow rate of 20 ml/min.

Thermogravimetric analysis (TGA) was performed using NETZSCH STA449F3 (NETZSCH-Gerätebau GmbH, Germany). The flame retardant (PBI) and the cured EP thermosets (approximately 7.0 mg) were put in an alumina crucible and heated from 40 °C to 700 °C at the heating rate of 10 °C/min under nitrogen or air atmosphere with a flow rate of 20 ml/min.

The LOI values were measured at room temperature on a JF-3 oxygen index meter (Jiangning Analysis Instrument Company, China) according to ASTM D2863 and dimensions of the cured EP thermosets were $100 \times 6.5 \times 3\ mm^3$. Vertical burning (UL-94) tests were carried out on the NK8017A instrument (Nklsky Instrument Co., Ltd., China) and dimensions of the cured EP thermosets were $130 \times 13 \times 3\ mm^3$ according to the UL-94 test standard.

Cone calorimeter measurements were performed on a FTT cone calorimeter according to the ISO 5660 standard under an external heat flux of 50 kW/m^2. Dimensions of the cured EP thermosets were $100 \times 100 \times 3\ mm^3$, and three specimens were tested for every sample.

Morphological studies on the residual chars after cone calorimeter test were conducted using a QuantaFEG450 (FEI, US) scanning electron microscope (SEM) at an acceleration voltage of 15 kV. The SEM instrument was integrated with an energy dispersive spectrometer (EDS) for elemental analysis using surface scanning model.

Pyrolysis-Gas Chromatography/Mass Spectrometry (Py-GC/MS) analysis was carried out with an Agilent 7890/5975 GC/MS (Agilent, US). The sample mass of PBI was about 2.0 mg. The injector temperature was 250 °C; 1 min at 50 °C then the temperature was increased to 280 °C at a rate of 8 °C/min. The temperature of the GC/MS interface was 280 °C, and the cracker temperature was 500 °C.

Thermogravimetric analysis/infrared spectrometry (TGA-FTIR) was performed on NETZSCH STA449F3 interfaced to the Nicolet 6700 FTIR spectrophotometer. FTIR was directly connected to TG and measured the gaseous decomposition products from TG by real time. PBI (approximately 7.0 mg) was put in an alumina crucible and heated from 40 °C to 700 °C at a heating rate of 10 °C/min under N_2 atmosphere with a flow rate of 20 ml/min.

3. Results and discussion

3.1. Characterization of PBI

The chemical structure of PBI was characterized by FTIR, HR-MS, ^1H and ^{31}P NMR. The corresponding data were shown in Fig. 1. As shown in Fig. 1(a), the FTIR spectrum of PBI showed several characteristic absorption peaks. The absorption peak at 3156 cm^{-1} was assigned to N–H [30]; the absorption peak at 1595 cm^{-1} was ascribed to the stretching vibration of C=N [36]; the absorption peak at 1529 cm^{-1} was assigned to benzene ring [36]; the absorption peak at 1445 cm^{-1} was assigned to the stretching vibration of C–N [29]; the absorption peak at 1205 was assigned to the stretching vibration of P=O [29,30]; the absorption peaks at 927 and 752 cm^{-1} were assigned to P–O-Ph linkage [24,36]. As shown in Fig. 1(b), The ^1H NMR spectrum of PBI showed the chemical shifts of aromatic hydrogen (including imidazole and benzene rings, 14H) at 6.8–8.3 ppm, C–H (methine, 1H) at 5.8–6.1 ppm, N–H (imino group linked with thiazole ring, 1H) at 8.5–9.0 ppm, N–H (imidazole ring, 1H) at 12.2–12.8 ppm. As shown in Fig. 1(c), the ^{31}P NMR spectrum of PBI showed two peaks at 29.1 and 29.6 ppm attributed to the phosphorus atom in DOPO group. As shown in Fig. 1(d), the *m/z* of PBI was 467.0694 $[M_+ Na]^+$, which was in accordance with the calculated molecular weight of PBI. Based on the above analyses, it was confirmed that PBI was successfully synthesized.

3.2. Curing behavior of the prepared EP curing systems

Non-isothermal DSC test was adopted to evaluate the influence of PBI on the curing behavior and cross-linked networks of EP systems. As shown in Fig. 2, EP/PBI system showed an exothermic interval during 130–150 °C. According to the chemical structure of PBI, it was considered that this exothermic interval was attributed to the addition reaction of epoxy group with N–H and anionic polymerization of epoxy groups initiated by the tertiary amine of imidazole and thiazole rings. EP/DDS system showed only one exothermic peak at 223 °C. However, with the incorporation of PBI, two exothermic peaks appeared. The main exothermic peaks of EP/DDS/PBI systems were attributed to the addition reaction between epoxy group and DDS, which were shifted to lower temperature region compared with that of EP/DDS system, indicating PBI accelerated the crosslinking reaction of DGEBA with DDS. This phenomenon was due to the tertiary amine of imidazole and thiazole rings, which could act as anion catalysis for epoxy ring opening. Moreover, with the increasing content of PBI, the small exothermic intervals of EP/DDS/PBI systems during 130–150 °C became more and more obvious. The result indicated the aforementioned chemical reactions in EP/PBI system also took place in EP/DDS/PBI systems despite of the presence of DDS. Therefore, PBI was chemically bonded with EP matrix to obtain intrinsic flame retardant thermosets. The proposed curing mechanism of EP/DDS/PBI systems was shown in Scheme 2.

3.3. Thermal properties

Based on the aforementioned discussion on curing behavior, it was known that PBI participated in the formation of EP cross-linked networks, thus it was meaningful to assess the effect of PBI on the glass transition behavior of EP thermosets. The glass transition temperature (T_g) of EP thermosets was investigated by DSC, as displayed in Fig. 3. The EP/DDS thermoset exhibited a high T_g value

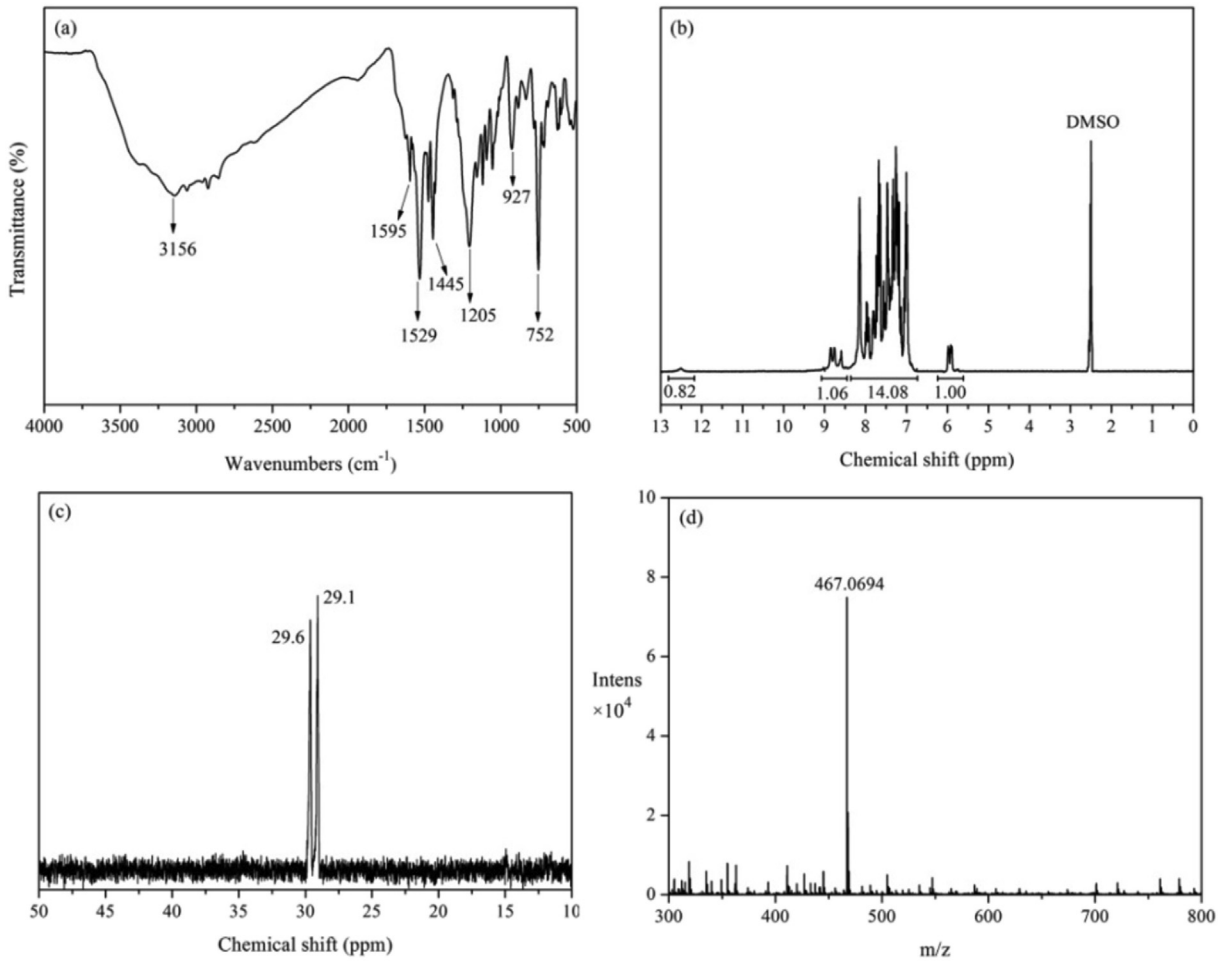

Fig. 1. FTIR (a), ^{1}H NMR (b), ^{31}P NMR (c) and MS (d) spectra of PBI.

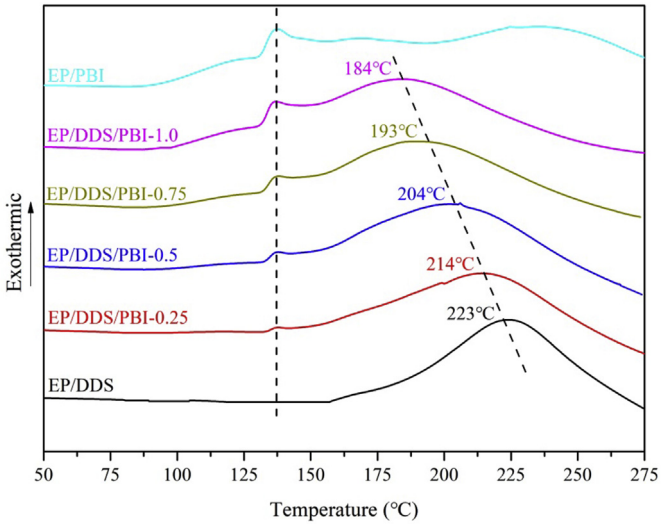

Fig. 2. Non-isothermal DSC curves of the prepared EP curing systems.

of 200 °C. With the incorporation of PBI, the T_g values of EP/DDS/PBI thermosets were decreased by 5–14 °C. On the one hand, PBI with two N–H bonds would act as chain extender during curing reaction, resulting in the decreased crosslinking density of epoxy thermosets. On the other hand, PBI with bulky rigid group increased the rotational barrier of macromolecular chain segments which compensated somewhat for the loss in crosslink density caused by chain extension reaction. These competing factors may be the reason why the T_g values of EP/DDS/PBI thermosets were just slightly decreased.

TGA was used to explore the thermal degradation behavior of PBI and EP thermosets under nitrogen and air atmospheres. The TG and DTG curves of PBI and EP thermosets were shown in Fig. 4. The relevant data, such as temperature at 5% weight loss ($T_{5\%}$), temperature at maximum weight loss rate (T_{max}) and char yields at 700 °C (Y_c) were listed in Table 2.

Firstly, the thermal degradation behavior of PBI and the prepared EP thermosets were investigated under nitrogen atmosphere. As shown in Fig. 4 (a), PBI was decomposed much earlier than the EP thermosets, which was attributed to the degradation of less thermally stable P–C and O=P–O bonds in PBI ahead of time [37]. All the EP thermosets exhibited one weight loss stage due to the decomposition of macromolecular networks. Compared with the EP/DDS thermoset, the $T_{5\%}$ and T_{max} of EP/DDS/PBI thermosets were gradually decreased with the increasing content of PBI. The lower initial decomposition temperatures of EP/DDS/PBI thermosets were ascribed to the lower thermal stability of PBI component. Moreover, the decomposition products of PBI accelerated the decomposition of EP matrix, resulting in remarkably decreased T_{max}. Notably, the Y_c values were significantly increased with the incorporation of PBI, indicating the decomposition products of PBI enhanced the charring ability of EP matrix.

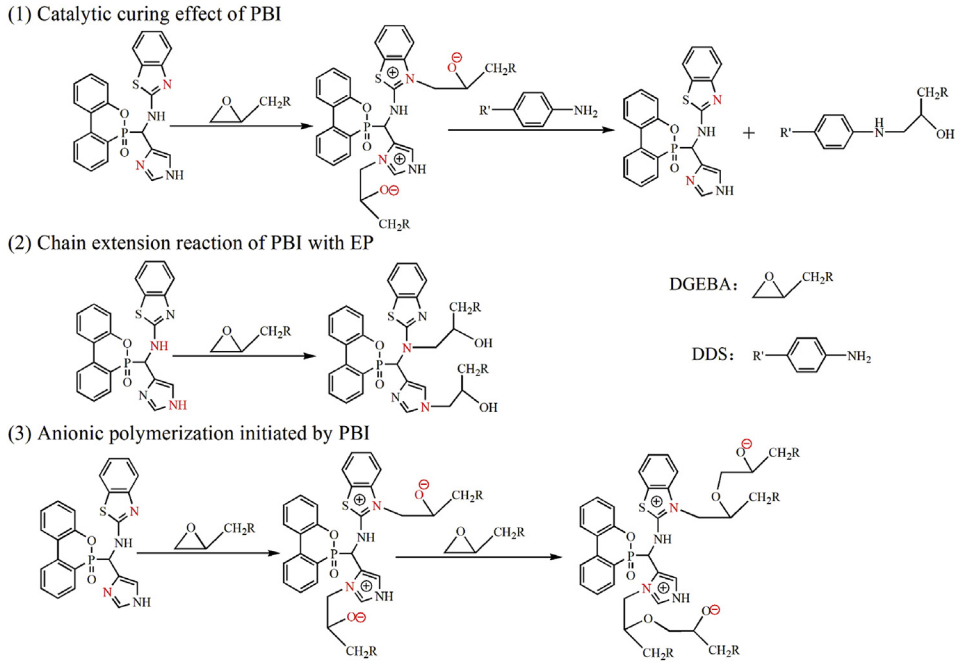

Scheme 2. The proposed curing mechanism of EP/DDS/PBI systems.

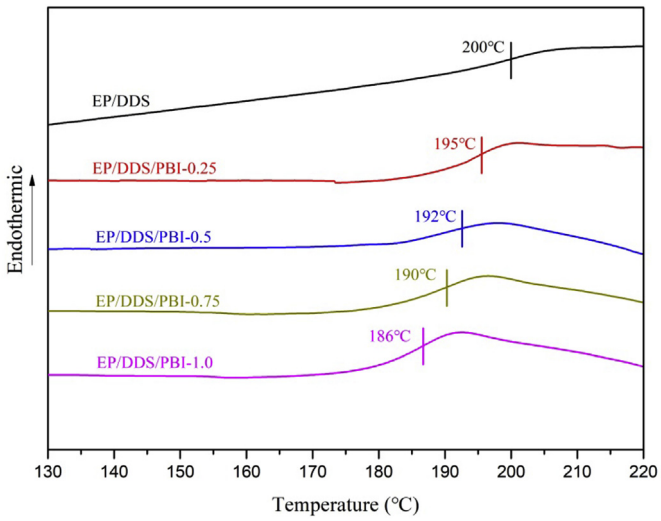

Fig. 3. DSC curves of the prepared EP thermosets.

In air atmosphere, as shown in Fig. 4 (c) and (d), all the EP thermosets exhibited two weight loss stages, which were corresponded to the degradation of macromolecular networks and further oxidation of char residues. Not surprisingly, the incorporation of PBI promoted the degradation of EP matrix as the case in nitrogen atmosphere. However, the $T_{5\%}$ and T_{max1} of EP/DDS/PBI thermosets were just slightly decreased, indicating the EP matrix maintained good thermal stability in air atmosphere despite of the incorporation of PBI. Moreover, the T_{max2} was gradually increased with the increasing content of PBI, indicating the formation of more stabilized char layers. It was deduced that PBI was decomposed to generate phosphorus-based acid which catalyzed the charring of EP matrix to form highly cross-linked char layers with better thermo-oxidative stability.

3.4. Flame retardant properties

The flame retardant effect of PBI on EP was initially investigated by LOI and UL94 tests. The related results were shown in Table 3. The EP/DDS thermoset was highly combustible with a LOI value of 22.5% and failed to pass UL94 test. With the incorporation of PBI, the flame retardancy of EP/DDS/PBI thermosets was remarkably enhanced. When the phosphorus content was only 0.25 wt%, The LOI value of EP/DDS/PBI-0.25 was raised to 28.8% though the sample still had no UL94 rating. As the phosphorus content further increased, EP/DDS/PBI thermosets performed better in both LOI and UL94 tests. When the phosphorus content was only 0.75 wt%, EP/DDS/PBI-0.75 had a LOI value of 34.6% and passed UL94 V-0 rating. The results revealed that PBI possesses excellent flame retardant effect on EP. It was worth noting that large amounts of noncombustible gases jetted out from the burning EP/DDS/PBI thermosets with a rush to extinguish the flame, namely blowing-out effect [34], as shown in Fig. 5. This phenomenon indicated an obvious flame retardant effect of PBI in gaseous phase.

In order to better study the influence of PBI on reducing the flammability of EP, cone calorimeter test was used to investigate the combustion behavior of the prepared EP thermosets. The corresponding parameters including the time to ignition (TTI), time of flameout (TOF), peak of heat release rate (pk-HRR), average of heat release rate (av-HRR), average of effective heat of combustion (av-EHC), average CO yield (av-COY), average CO_2 yield (av-CO_2Y) and residual weight were listed in Table 3. The averages were recorded during TTI to 500 s.

The curves of heat release rate (HRR) and total heat release (THR) were shown in Fig. 6. The EP/DDS thermoset burned fiercely after ignition and its HRR reached a sharp peak with a pk-HRR value of 1208 kW/m^2. With the incorporation of PBI, the EP/DDS/PBI thermosets were ignited earlier compared with the EP/DDS thermoset. As a DOPO based flame retardant, PBI induced the decomposition of EP matrix in advance, thus weakening the ignition resistance [29,36]. Moreover, the pk-HRR, av-HRR and THR values of EP/DDS/PBI-1.0 thermoset were reduced by 49.5%, 36.2% and

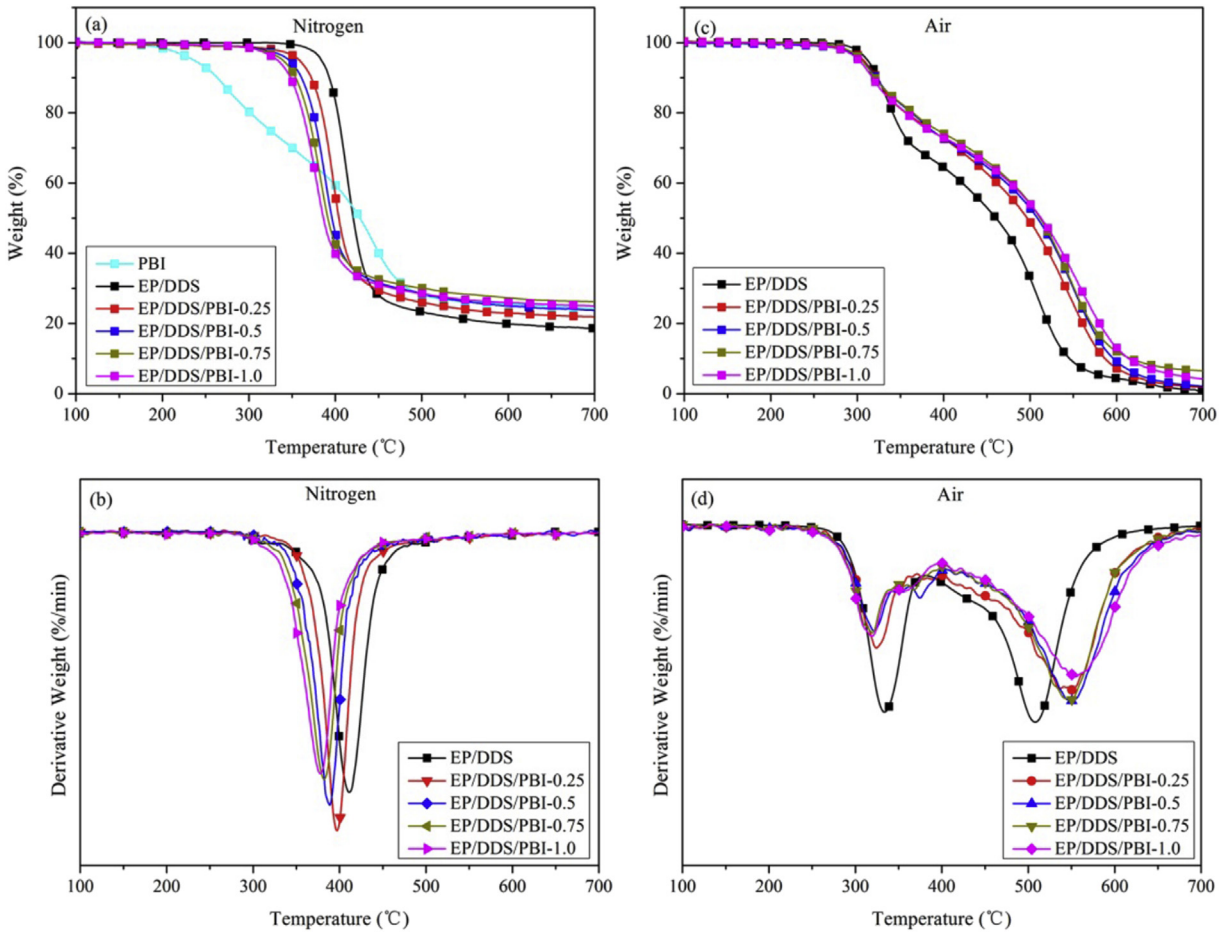

Fig. 4. TGA and DTG curves of PBI and the prepared EP thermosets under nitrogen and air atmospheres.

Table 2
TGA data of PBI and the prepared EP thermosets.

Sample code	Nitrogen			Air			
	$T_{5\%}$ (°C)	T_{max} (°C)	Y_c (%)	$T_{5\%}$ (°C)	T_{max1} (°C)	T_{max2} (°C)	Y_c (%)
PBI	237	–	24.3	–	–	–	–
EP/DDS	384	411	18.6	308	332	507	0.8
EP/DDS/PBI-0.25	359	396	21.9	304	324	536	1.9
EP/DDS/PBI-0.5	345	388	24.1	303	321	549	2.1
EP/DDS/PBI-0.75	339	382	26.2	302	319	550	6.5
EP/DDS/PBI-1.0	333	378	25.0	300	318	555	4.2

Table 3
LOI, UL94 and cone calorimeter results for the prepared EP thermosets.

Sample	LOI (%)	UL94 (3 mm)	TTI/TOF (s)	pk-HRR (kW/m^2)	av-HRR (kW/m^2)	av-EHC (MJ/kg)	av-COY (kg/kg)	av-CO_2Y (kg/kg)	Residual weight (%)
EP/DDS	22.5	NR	47/430	1208	177	22.2	0.063	1.589	10.4
EP/DDS/PBI-0.25	28.8	NR	45/219	1046	152	19.5	0.075	1.265	15.7
EP/DDS/PBI-0.5	31.4	V-1	35/209	922	146	19.1	0.089	1.202	17.5
EP/DDS/PBI-0.75	34.6	V-0	31/207	620	122	18.1	0.122	1.106	21.8
EP/DDS/PBI-1.0	33.5	V-0	23/160	610	113	18.2	0.158	1.025	21.2

33.0%, respectively, in comparison with those of the EP/DDS thermoset. The results strongly demonstrated the combustion intensity of EP matrix was remarkably suppressed with the incorporation of PBI.

Av-EHC, which is the ratio of average of heat release rate (av-HRR) to the average mass loss rate from the cone calorimetry test, discloses the burning rate of volatile gases in gaseous phase flame during combustion. As shown in Table 3, the obviously decreased av-EHC values of EP/DDS/PBI thermosets indicated the incomplete combustion and flame retardant effect in gaseous phase with the

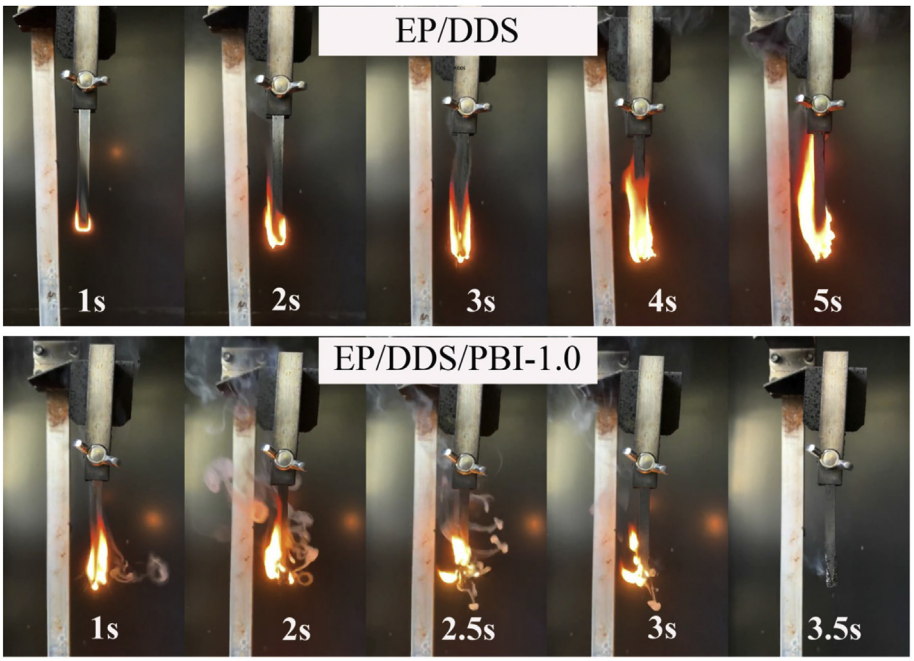

Fig. 5. Video screenshots of the EP/DDS and EP/DDS/PBI-1.0 thermosets during UL94 test.

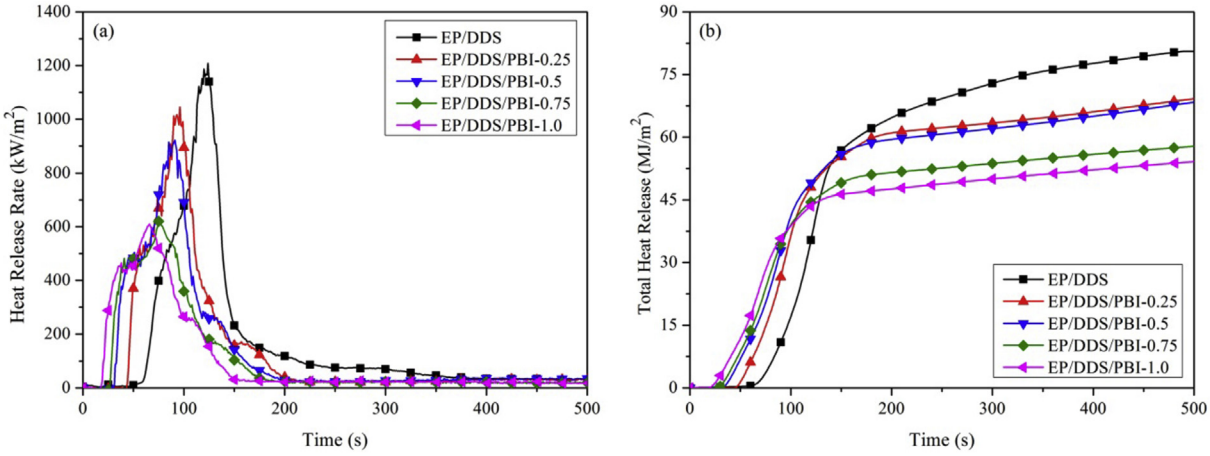

Fig. 6. HRR (a) and THR (b) curves of the prepared EP thermosets.

presence of PBI. The result was further proved by TOF, av-COY, and av-CO_2Y. As shown in Table 3, EP/DDS/PBI thermosets were more easily extinguished and their TOF values were shortened to a large extent compared with the EP/DDS thermoset. In addition, the av-COY increased whereas the av-CO_2Y decreased with the addition of PBI. More av-COY and less av-CO_2Y meant more incomplete combustion products (CO) and less complete combustion products (CO_2) [29]. It was inferred that PBI was decomposed to release pyrolysis fragments with quenching effect in gaseous phase during combustion. Furthermore, it was found that the EP/DDS/PBI thermosets exhibited much higher residual weight (Table 3) which was in accordance with TGA results, strongly demonstrating the flame retardant effect of PBI in condensed phase. From what had been discussed above, it was considered that the flame retardant effect of PBI in both gaseous and condensed phases was responsible for the significantly enhanced flame retardancy of EP/DDS/PBI thermosets. The flame retardant mechanism was further investigated in the subsequent sections.

3.5. Morphology and chemical analysis of char residues

In order to further illuminate the flame retardant mechanism in condensed phase, the morphology and chemical structure of the char residues derived from cone calorimeter test were investigated.

Not surprisingly, the EP/DDS thermoset was almost burnt out, leaving very few char residue with a fragmentized and collapsed structure, as shown in Fig. 7. However, the char residue of EP/DDS/PBI-1.0 thermoset exhibited a more dense, continuous and intumescent structure. The SEM images of the exterior and interior char residues of EP/DDS/PBI-1.0 thermoset showed a continuous and enclosed surface with honeycomb-like structure inside. Beyond doubt, this kind of char structure contributed to preventing the release of gaseous fuels into the gaseous phase and reducing the heat- and oxygen-exchange efficiency.

The FTIR spectra of the char residues were shown in Fig. 8. As shown in Fig. 8, the absorption peaks at 1594, 1509 and 829 cm^{-1} indicated the formation of polyaromatic carbons [26]. What's more,

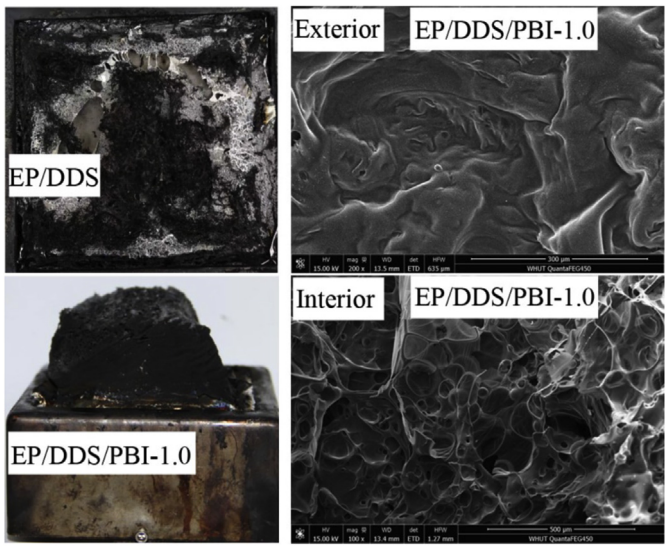

Fig. 7. The digital and SEM images of the char residues.

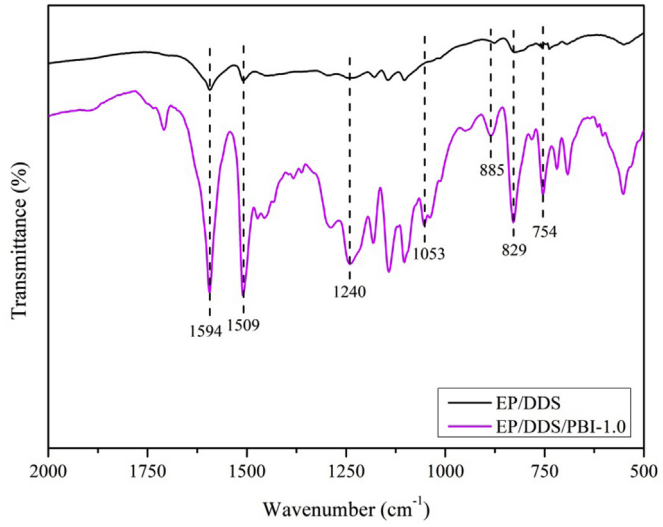

Fig. 8. The FTIR spectra of the char residues.

some new absorption peaks emerged in the FTIR spectrum of EP/DDS/PBI-1.0. The absorption peak at 1240 cm^{-1} was assigned to P═O [30]; the absorption peaks at 1053, 885 and 754 cm^{-1} indicated the formation of P–O–P and P–O–C [36]. The elementary compositions of the char residues were investigated by EDS under surface scanning model. The EDS results were shown in Fig. 9. For the char residue of the EP/DDS thermoset, the main composition of the residue was carbon, while the phosphorus and oxygen contents were significantly increased for the char residue of EP/DDS/PBI-1.0 thermoset. The above results provided the direct evidence that PBI was decomposed to form phosphorus-containing fragments which combined with oxygen to generate phosphate and the related analogues during combustion. These organophosphorus compounds were responsible for the enhanced charring ability of EP matrix.

3.6. Pyrolysis behavior

Phosphorus/nitrogen-containing compounds always exerted flame retardant action in gaseous phase by releasing pyrolysis products with quenching and diluting effects. To gain insight into the flame retardant mechanism in gaseous phase, the pyrolysis products of PBI were detected using TG-FTIR and Py-GC/MS.

The FTIR spectra at different temperatures selected from the TG-FTIR test were shown in Fig. 10. As shown in Fig. 10, the absorption peak at 3900-3500 cm^{-1} assigned to OH [24], 3070 cm^{-1}ascribed to aromatic hydrogen [30] and 1615 and 1455 cm^{-1} due to the skeletal vibration of benzene ring [26] indicated the presence of phenols fragments during the decomposition of PBI. The absorption peak at 1712 $cm^{-1}$was assigned to C═O [24]; the absorption peaks at 1540, 1377, 964 and 930 cm^{-1}were assigned to S═C═S, C–N and NH_3 [24,30], respectively, owing to the decomposition of imidazole and aminothiazole groups. The absorption peaks of P═O at 1290 cm^{-1}, P–O–P at 1096 cm^{-1}, P–O–C at 754 and 870 cm^{-1} suggested the decomposition of DOPO group [24,30].

The pyrolysis behavior of PBI was further investigated by Py-GC/MS test. The total ion chromatogram (TIC) was shown in Fig. 11. It was obvious that the TIC exhibited several small peaks and a strong peak during 14.8–17.0 min, and accordingly the typical MS spectra at different retention time were also provided. The characteristic fragment ions identified from the Py-GC/MS spectra of PBI were shown in Fig. 12. The *m*/*z* of fragments at 40, 41, 66 and 67 were attributed to the decomposition of imidazole moiety of PBI. The *m*/*z* of fragments at 93 and 94 was attributed to phenoxyl free radical and phenol [29]; the *m*/*z* of fragment at 215 was identified as

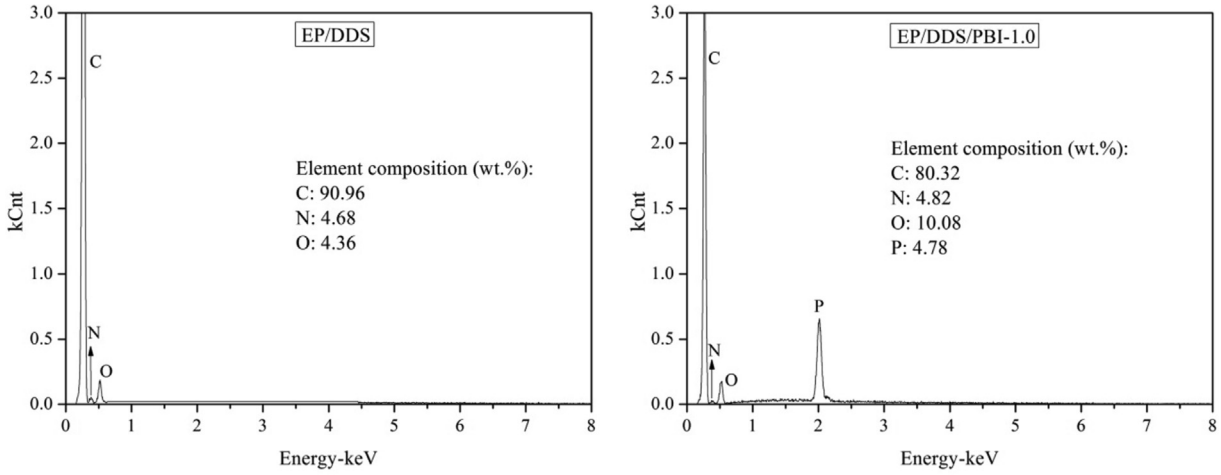

Fig. 9. The EDS results of the char residues.

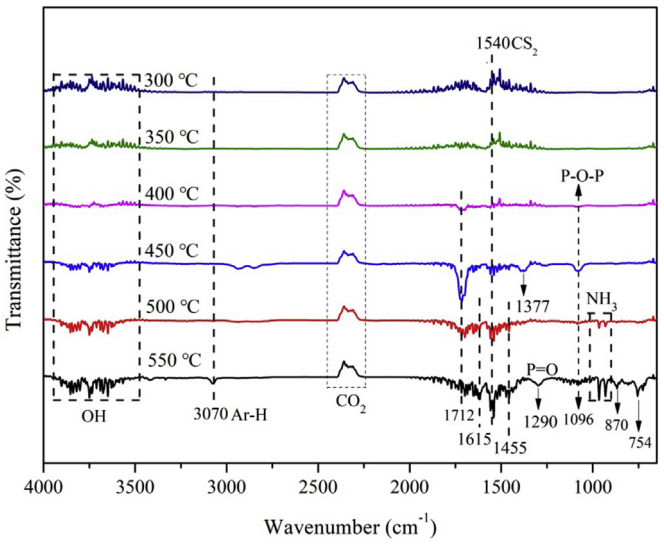

Fig. 10. The FTIR spectra of the volatile products of PBI at different temperatures.

phosphaphenanthrene group [29]; the *m*/*z* of fragments at 63 and 64 were considered as PO_2 free radical and HPO_2 produced by the PO free radicals from the broken phosphaphenanthrene group combining with OH, H, or O free radicals [22]; the *m*/*z* of fragments at 168, 169 and 170 are determined as dibenzofuran, o-phenylphenoxyl free radical, and o-phenylphenol, respectively [22,29]. The *m*/*z* of fragment at 139 and 141 were considered as the O═P—O—Ph free radicals [24]. The *m*/*z* of fragments at 149 and 150 were identified as aminobenzothiazole free radical and 2-aminobenzothiazole; the *m*/*z* of fragments at 44, 123, 124, 135, 151and 152 were assigned to the decomposition products of benzothiazole group of PBI. The above results strongly demonstrated the phosphorus-containing free radicals with quenching effect and nonflammable nitrogen- and sulphur-containing fragments with diluting effect were produced during the thermal decomposition process of PBI. The Py-GC/MS results were well in accordance with the TG-FTIR results.

According to the above analyses, the flame retardant mechanism was concluded as follows. During combustion, the DOPO group of PBI was decomposed form phosphorus-containing fragments. Thereinto, some phosphorus-containing fragments were released to the gaseous phase and were capable of quenching the H• and •OH free radicals; the other phosphorus-containing fragments were maintained in condensed phase to form phosphate and the related analogues which could catalyze the charring of EP matrix to form protective char layer with high char yield [17]. In addition, the imidazole and benzothiazole groups of PBI were decomposed to release noncombustible gases with diluting effect. Furthermore, the blowing-out effect was observed when large amounts of noncombustible gases and phosphorous-containing radicals jetted out with a rush from the surface of the burning matrix.

4. Conclusion

In this work, a DOPO based reactive flame retardant (PBI) composed of multiple heteroaromatic groups was synthesized and used as flame retardant co-curing agent for EP. PBI accelerated the crosslinking reaction of EP and participated in the formation of cross-linked networks. The T_g values of the resulting EP thermosets were only slightly decreased with the incorporation of PBI. PBI exerted both the catalytic decomposition and catalytic charring effects on EP. The combustion test results demonstrated the flame retardancy of EP thermosets was remarkably enhanced with the incorporation of PBI. When the phosphorus content was only

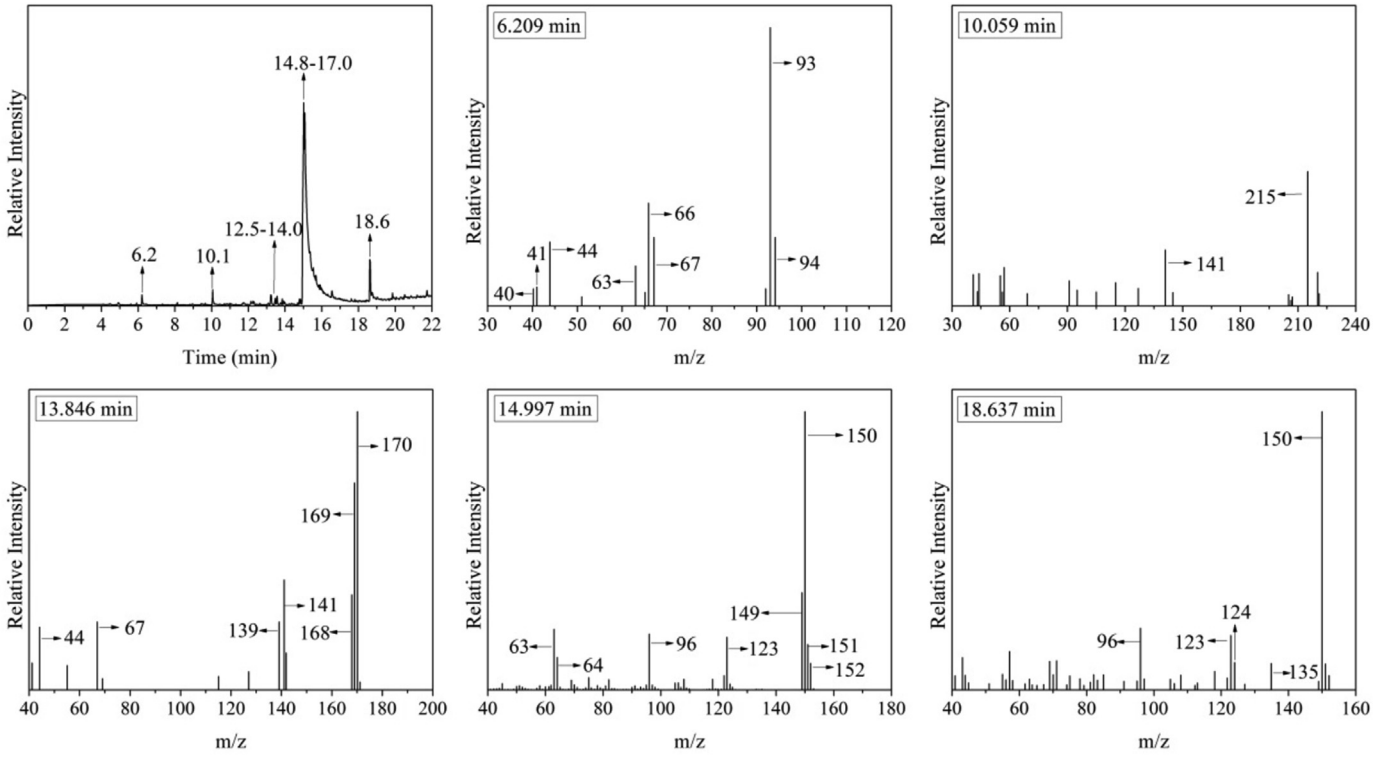

Fig. 11. The TIC and typical Py-GC/MS spectra for PBI.

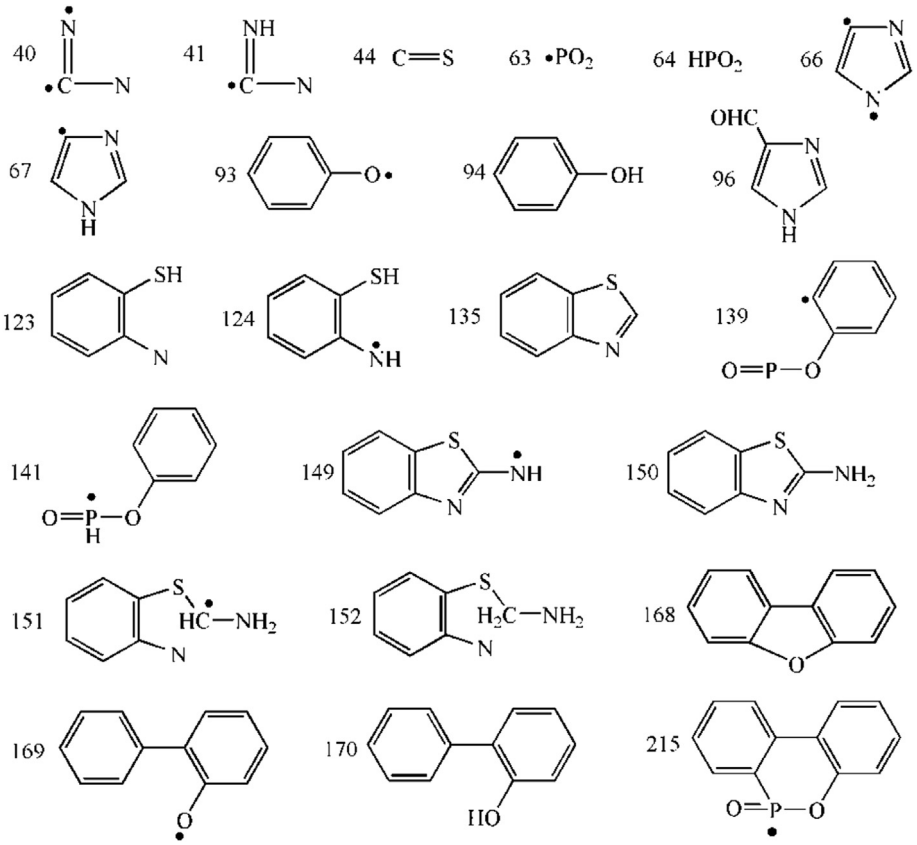

Fig. 12. The characteristic fragment ions identified from the Py-GC/MS spectra of PBI.

0.75 wt%, EP/DDS/PBI-0.75 thermoset achieved a LOI value of 34.6% and passed UL94 V-0 rating. Moreover, the pk-HRR, av-HRR and THR values were decreased by 48.7%, 31.1% and 28.3%, respectively, in comparison with those of the EP/DDS thermoset. The investigation on flame retardant mechanism revealed the bi-phase flame retardant effect of PBI on EP.

Acknowledgements

This work was supported by “the National Natural Science Foundation of China” (Grant Numbers 51803159 and 51775400).

References

[1] P. Müller, M. Morys, A. Sut, C. Jäger, B. Illerhaus, B. Schartel, Melamine poly(zinc phosphate) as flame retardant in epoxy resin: decomposition pathways, molecular mechanisms and morphology of fire residues, Polym. Degrad. Stabil. 130 (2016) 307–319.
[2] P. Müller, B. Schartel, Melamine poly (metal phosphates) as flame retardant in epoxy resin: performance, modes of action, and synergy, J. Appl. Polym. Sci. 133 (2016).
[3] E. Cechova, S. Vojta, P. Kukucka, A. Kocan, T. Trnovec, L.P. Murinova, et al., Legacy and alternative halogenated flame retardants in human milk in Europe: implications for children's health, Environ. Int. 108 (2017) 137–145.
[4] Y.L. Wei, L.J. Bao, C.C. Wu, E.Y. Zeng, Characterization of anthropogenic impacts in a large urban center by examining the spatial distribution of halogenated flame retardants, Environ. Pollut. 215 (2016) 187–194.
[5] S.Y. Lu, I. Hamerton, Recent developments in the chemistry of halogen-free flame retardant polymers, Prog. Polym. Sci. 27 (2002) 1661–1712.
[6] M. Rakotomalala, S. Wagner, M. Doring, Recent developments in halogen free flame retardants for epoxy resins for electrical and electronic applications, Materials 3 (2010) 4300–4327.
[7] C. Ma, B. Yu, N.N. Hong, Y. Pan, W.Z. Hu, Y. Hu, Facile synthesis of a highly efficient, halogen-free, and intumescent flame retardant for epoxy resins: thermal properties, combustion behaviors, and flame-retardant mechanisms, Ind. Eng. Chem. Res. 55 (2016) 10868–10879.
[8] M. Ciesielski, B. Burk, C. Heinzmann, M. Döring, Fire-retardant High-Performance Epoxy-Based Materials. Novel Fire Retardant Polymers and Composite Materials, Elsevier, 2017, pp. 3–51.
[9] B. Schartel, Phosphorus-based flame retardancy mechanisms-old hat or a starting point for future development? Materials 3 (2010) 4710–4745.
[10] C. Schmidt, M. Ciesielski, L. Greiner, M. Doring, Novel organophosphorus flame retardants and their synergistic application in novolac epoxy resin, Polym. Degrad. Stabil. 158 (2018) 190–201.
[11] S. Liu, B. Yu, Y. Feng, Z. Yang, B. Yin, Synthesis of a multifunctional bisphosphate and its flame retardant application in epoxy resin, Polym. Degrad. Stabil. 165 (2019) 92–100.
[12] B.A. Howell, A. Alrubayyi, 2-Dopyl-1,4-di(2-dopylpropanoyl)benzene, an effective phosphorus flame retardant, Polym. Degrad. Stabil. 162 (2019) 196–200.
[13] Z.M. Zhu, L.X. Wang, L.P. Dong, Influence of a novel P/N-containing oligomer on flame retardancy and thermal degradation of intumescent flame-retardant epoxy resin, Polym. Degrad. Stabil. 162 (2019) 129–137.
[14] B. Schartel, A.I. Balabanovich, U. Braun, U. Knoll, J. Artner, M. Ciesielski, et al., Pyrolysis of epoxy resins and fire behavior of epoxy resin composites flame-retarded with 9,10-dihydro-9-oxa-10-phosphaphenanthrene-10-oxide additives, J. Appl. Polym. Sci. 104 (2007) 2260–2269.
[15] M. Ciesielski, A. Schafer, M. Doring, Novel efficient DOPO-based flame-retardants for PWB relevant epoxy resins with high glass transition temperatures, Polym. Adv. Technol. 19 (2008) 507–515.
[16] B. Perret, B. Schartel, K. Stoss, M. Ciesielski, J. Diederichs, M. Doring, et al., Novel DOPO-based flame retardants in high-performance carbon fibre epoxy composites for aviation, Eur. Polym. J. 47 (2011) 1081–1089.
[17] B. Schartel, B. Perret, B. Dittrich, M. Ciesielski, J. Kramer, P. Muller, et al., Flame retardancy of polymers: the role of specific reactions in the condensed phase, Macromol. Mater. Eng. 301 (2016) 9–35.
[18] K.A. Salmeia, S. Gaan, An overview of some recent advances in DOPO-derivatives: chemistry and flame retardant applications, Polym. Degrad. Stabil. 113 (2015) 119–134.
[19] J. Artner, M. Ciesielski, O. Walter, M. Doring, R.M. Perez, J.K.W. Sandler, et al., A novel DOPO-based diamine as hardener and flame retardant for epoxy resin systems, Macromol. Mater. Eng. 293 (2008) 503–514.
[20] B. Perret, B. Schartel, K. Stöß, M. Ciesielski, J. Diederichs, M. Döring, et al., A new halogen-free flame retardant based on 9, 10-Dihydro-9-oxa-10-phosphaphenanthrene-10-oxide for epoxy resins and their carbon fiber composites for the automotive and aviation industries, Macromol. Mater. Eng. 296 (2011) 14–30.

[21] M.-J. Xu, G.-R. Xu, Y. Leng, B. Li, Synthesis of a novel flame retardant based on cyclotriphosphazene and DOPO groups and its application in epoxy resins, Polym. Degrad. Stabil. 123 (2016) 105–114.
[22] L. Qian, L. Ye, Y. Qiu, S. Qu, Thermal degradation behavior of the compound containing phosphaphenanthrene and phosphazene groups and its flame retardant mechanism on epoxy resin, Polymer 52 (2011) 5486–5493.
[23] L.-J. Qian, L.-J. Ye, G.-Z. Xu, J. Liu, J.-Q. Guo, The non-halogen flame retardant epoxy resin based on a novel compound with phosphaphenanthrene and cyclotriphosphazene double functional groups, Polym. Degrad. Stabil. 96 (2011) 1118–1124.
[24] S. Yang, J. Wang, S. Huo, M. Wang, L. Cheng, Synthesis of a phosphorus/nitrogen-containing additive with multifunctional groups and its flame-retardant effect in epoxy resin, Ind. Eng. Chem. Res. 54 (2015) 7777–7786.
[25] L. Qian, Y. Qiu, J. Liu, F. Xin, Y. Chen, The flame retardant group-synergistic-effect of a phosphaphenanthrene and triazine double-group compound in epoxy resin, J. Appl. Polym. Sci. 131 (2014).
[26] S. Yang, J. Wang, S.Q. Huo, L.F. Cheng, M. Wang, Preparation and flame retardancy of an intumescent flame-retardant epoxy resin system constructed by multiple flame-retardant compositions containing phosphorus and nitrogen heterocycle, Polym. Degrad. Stabil. 119 (2015) 251–259.
[27] S. Yang, J. Wang, S.Q. Huo, L.F. Cheng, M. Wang, The synergistic effect of maleimide and phosphaphenanthrene groups on a reactive flame-retarded epoxy resin system, Polym. Degrad. Stabil. 115 (2015) 63–69.
[28] S. Tang, L.J. Qian, X.X. Liu, Y.P. Dong, Gas-phase flame-retardant effects of a bi-group compound based on phosphaphenanthrene and triazine-trione groups in epoxy resin, Polym. Degrad. Stabil. 133 (2016) 350–357.
[29] L.J. Qian, Y. Qiu, N. Sun, M.L. Xu, G.Z. Xu, F. Xin, et al., Pyrolysis route of a novel flame retardant constructed by phosphaphenanthrene and triazine-trione groups and its flame-retardant effect on epoxy resin, Polym. Degrad. Stabil. 107 (2014) 98–105.
[30] R.K. Jian, P. Wang, L. Xia, X. Zheng, Effect of a novel P/N/S-containing reactive flame retardant on curing behavior, thermal and flame-retardant properties of epoxy resin, J. Anal. Appl. Pyrolysis 127 (2017) 360–368.
[31] Y. Zhang, B. Yu, B.B. Wang, K.M. Liew, L. Song, C.M. Wang, et al., Highly effective P-P synergy of a novel DOPO-based flame retardant for epoxy resin, Ind. Eng. Chem. Res. 56 (2017) 1245–1255.
[32] W.C. Zhang, A. Fina, G. Ferraro, R.J. Yang, FTIR and GCMS analysis of epoxy resin decomposition products feeding the flame during UL 94 standard flammability test. Application to the understanding of the blowing-out effect in epoxy/polyhedral silsesquioxane formulations, J. Anal. Appl. Pyrolysis 135 (2018) 271–280.
[33] W.C. Zhang, X.M. Li, R.J. Yang, Study on the change of silicon and phosphorus content in the condensed phase during the combustion of epoxy resin with OPS/DOPO, Polym. Degrad. Stabil. 99 (2014) 298–303.
[34] W.C. Zhang, X.M. Li, R.J. Yang, Novel flame retardancy effects of DOPO-POSS on epoxy resins, Polym. Degrad. Stabil. 96 (2011) 2167–2173.
[35] Y. Qiu, L.J. Qian, H.S. Feng, S.L. Jin, J.W. Hao, Toughening effect and flame-retardant behaviors of phosphaphenanthrene/phenylsiloxane bigroup macromolecules in epoxy thermoset, Macromolecules 51 (2018) 9992–10002.
[36] S.Q. Huo, J. Wang, S. Yang, C. Li, X.L. Wang, H.P. Cai, Synthesis of a DOPO-containing imidazole curing agent and its application in reactive flame retarded epoxy resin, Polym. Degrad. Stabil. 159 (2019) 79–89.
[37] P. Wang, L. Chen, H. Xiao, Flame retardant effect and mechanism of a novel DOPO based tetrazole derivative on epoxy resin, J. Anal. Appl. Pyrolysis 139 (2019) 104–113.